



# Radiated sound power estimates of building elements by means of laser Doppler vibrometry

N.B. Roozen<sup>1</sup>, L. Labelle<sup>1</sup>, M. Rychtáriková<sup>1,2</sup>, C. Glorieux<sup>1</sup>, D. Urbán<sup>3</sup>, P. Zátka<sup>3</sup>, H. Mullner<sup>4</sup>

<sup>1</sup>Laboratory of Acoustics, Div. Soft Matter and Biophysics, Dep. Physics and Astronomy, KU Leuven, Belgium

<sup>2</sup>STU Bratislava, Fac. Civil Engineering, Dep. Building Structures, Radlinského 11, Bratislava, Slovak Republic

<sup>3</sup>A&Z Acoustics s.r.o., Repašského 2, 84102 Bratislava, Slovakia

<sup>4</sup>Federal Institute of Technology TGM, Department of Acoustics and Building Physics, Vienna, Austria

## Abstract

The measurement of the sound reduction index  $R$  of building elements is typically performed according to ISO 10140, by measuring the sound pressure level in the sending and receiving room, using standardized loudspeaker-microphone instrumentation. Recent proposals for new building acoustic standards taking into account frequencies down to 50 Hz, provoke new questions. At low frequencies (depending on the dimensions of the rooms), the modal density in the rooms is typically too low, impeding reliable measurements following standard techniques. In this paper, laser Doppler vibrometry is introduced as an alternative approach for the lower frequency region, to determine the intrinsic sound transmission properties of a building element, independently of the particular properties of the test facility. In addition, laser Doppler vibrometry offers the additional advantage in that it can identify the actual boundary conditions of a building element, which can be useful for modeling and prediction of the performance of building acoustics applications. A number of applications will be given.

## 1 Introduction

A standardized manner to determine the sound reduction index  $R$  of a building element in laboratory conditions, is described in ISO 10140:2010. It is known that the acoustic characteristics of the transmission suite can influence the measured sound reduction index, [1, 2] especially at low frequencies. More specifically, a large uncertainty of the sound insulation of a test wall is caused by two factors. One factor is a measurement uncertainty, which is caused by the fact that at low frequencies the pressure fields in the receiving room (and sending room) varies significantly in space. A second aspect is caused by the modal coupling between modes in the source room and the modes of the partition being tested. At low frequencies this aspect makes that the radiated active acoustic power is significantly affected at the modal resonance frequencies of the receiving room, as will be explained later in this paper.

In this paper the vibrational response of a building element in a transmission facility, is used to determine the radiated sound power of the walls [3]. The response is determined by advanced scanning LDV measurements. The input boundary condition is obtained from numerical algorithms, that use the spatial distribution of the velocity along the surface of the vibrating building element. Two walls are considered, and results are compared with standardized microphone approaches.

In addition to that, the influence of panel fastening on the acoustic performance of lightweight building elements is assessed by means of LDV [4]. Using the LDV approach the reason of the acoustic performance difference could physically be explained.

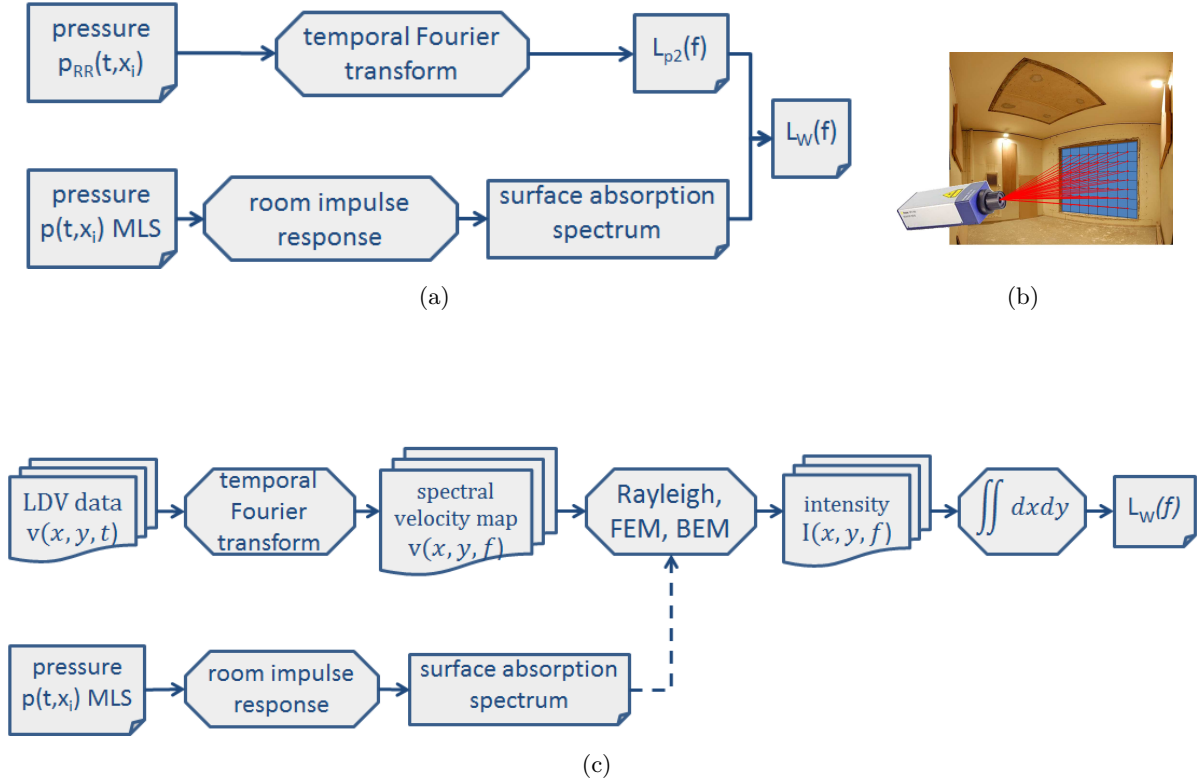


Figure 1: Methodologies to determine radiated sound power. (a) Microphone based ISO 10140. (b) Illustration of laser Doppler based approach (c) Laser Doppler based approach.

## 2 Determination of radiated sound power by laser Doppler vibrometry.

A methodology is proposed to determine the radiated sound power from laser Doppler vibrometry measurements of the vibrating wall, as an alternative for the methodology described in ISO 3741:2010. The sound power, which is radiated by the vibrating wall into the receiving room is calculated from the measured vibration data by means of a Rayleigh integral model. To this end, the pressure on the surface of the vibrating wall is calculated, which, when combined with the (known) velocity of the vibrating wall, yields the sound intensity in normal direction to the wall. Integrating the sound intensity across the wall gives the radiated sound power. This measurement methodology is depicted graphically in Figure 1(c), and illustrated in Figure 1(b). For further details see [3].

### 2.1 Measurement set-up.

Experiments were performed in the transmission suite of the Laboratory of Acoustics of KU Leuven. The sending and receiving room are separated by a slightly inclined test partition. The Schroeder frequency of the rooms is approximately 350 [Hz].

A lightweight double wall was measured, consisting of two gypsum board plates, each with a thickness of 15mm. The plates were separated by an air gap with a thickness of 75 mm, which was filled with mineral wool. The double wall panel was supported by means of five vertically placed aluminum studs, placed in between the two gypsum board panels, every 60cm.

The test wall was excited by a sound field that was generated in the source room, by two sound sources emitting random pink noise, 95 dB in each  $1/3^{rd}$  octave band. The responses were measured by means of a scanning system. For further details see [3].

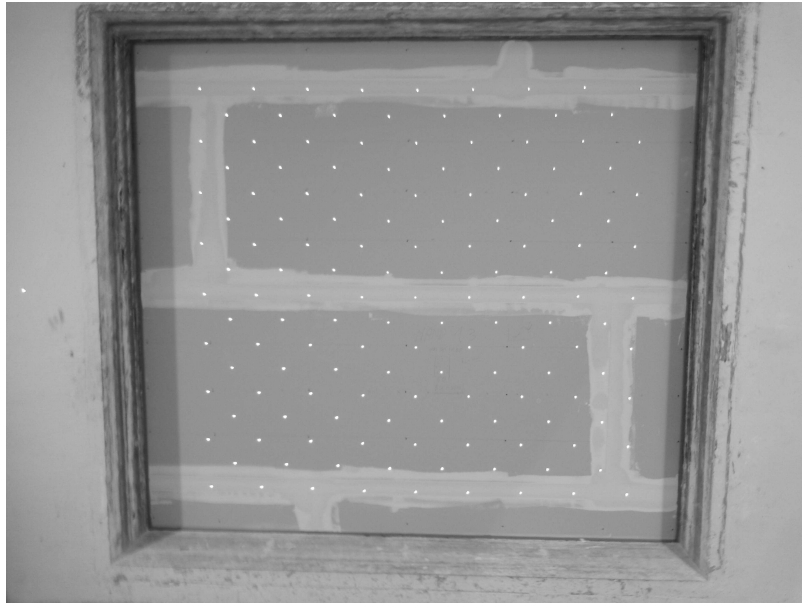


Figure 2: Lightweight double wall mounted in the transmission suite.

## 2.2 Determination of radiated sound power by Laser Doppler vibrometry

The radiated sound power was calculated from LDV measurement data using BEM/FEM simulations and a Rayleigh integral approach. BEM simulations were performed for the lightweight double wall case, with a frequency resolution of 0.05 Hz (corresponding to the frequency resolution at which the LDV measurements were performed). This frequency resolution was more than sufficient to accurately capture the structural and acoustic resonances. Results of the BEM simulations are shown in Fig. 3. In the simulations a complex speed of sound was used, where the imaginary part of the speed of sound was based on the reverberation time measurements (see [3] for further details). The narrowband estimates of the radiated active sound power which is based upon the Rayleigh integral, and the spatially averaged vibration spectrum of the test wall, are shown in Fig. 3 as well.

The differences in the sound power levels as estimated by the Rayleigh integral and BEM approach, clearly quantify the influence of the transmission suite due to modal effects of the receiving room. For instance, at a frequency of 66.8 Hz, the BEM-model estimates a rather sharp peak in the sound power level, whilst the Rayleigh-integral does not show a peak. Many other examples of this situation can be found, e.g. at 33.5 Hz, 39.1 Hz, 41.2 Hz, 53.1 Hz, 57.7 Hz, 78.6 Hz, 82.8 Hz and 92.2 Hz, indicated in Fig. 3 by means of vertical dotted lines (in blue color). All these frequencies correspond to acoustic resonance frequencies of the receiving room. The eigenmodes of the receiving room up to 70 Hz, as calculated by means of a FEM model, are presented in Fig. 4.

The active sound power that is radiated by the building element into the receiving room is larger at acoustic resonances of the receiving room. This is due to the fact that the acoustic impedance that is felt by the vibrating wall is much larger at acoustic resonance frequencies of the receiving room as compared to non-resonant frequencies. This causes the radiated active sound power of a panel to be dependent on the dimensions of the receiving room.

A comparison of laser Doppler vibrometry based sound power levels and conventionally determined sound power levels appeared to converge to each other at the higher frequencies, where the receiving room acoustics is diffuse. See [3] for further details.

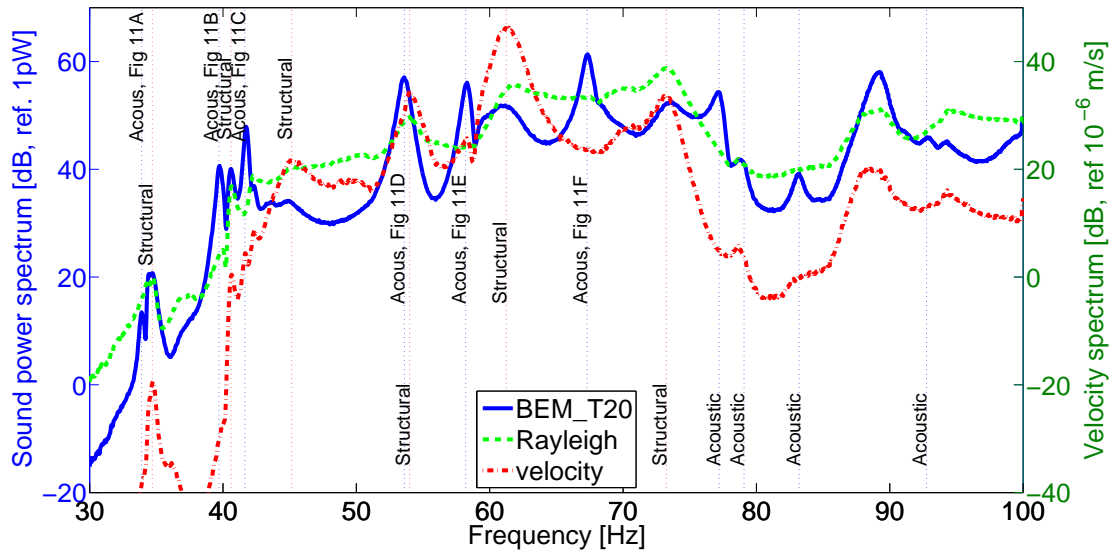


Figure 3: Radiated active sound power levels of the lightweight wall depicted in a spectrum with high resolution ( $\Delta f=0.05\text{Hz}$ ). Solid blue curve: BEM, damping parameter  $\xi$  based on  $T_{20}$ . Dashed green curve: Rayleigh-integral. Dashed-dotted red curve: Spatially averaged velocity of test panel.

### 3 Influence of panel fastening on the acoustic performance of light-weight structures.

It is known that workmanship concerning the fastening of the panels has significant influence on the sound insulation characteristics of lightweight construction building elements, e.g. timber frame partitions. The used method to fasten (e.g. with screws or staples) the panel (e.g. gypsum boards, gypsum fiber boards or chipboards) to the studs has a considerable influence on the sound insulation characteristics, and thus on the single values that are commonly used for rating the acoustic insulation performance.

In this article the effect of the number of screws, (and in [4] also how firmly the panel is fastened to the studs), on the sound reduction index  $R$  of the lightweight building element was studied experimentally. Standardized sound insulation measurements according to ISO 10140 were carried out and supported by scanning laser Doppler vibrometer (LDV) measurements. In this paper only two configurations will be discussed. For a discussion of all configurations measured, reference is made to [4] for a discussion of all configurations.

#### 3.1 Test wall measurement set-up.

The test specimen was mounted into the test opening with dimensions 2770 mm (height) and 3710 mm (width) (total surface area of  $10.4\text{ m}^2$ ) of the measurement facilities of TGM, Vienna, Austria. The timber frame consisted of timber studs of 160 mm / 80 mm section. The studs were mounted 625 mm off-centre distance to each other. On both sides 12.5 mm gypsum fiber boards (three in total on each side) with dimensions of 2760 mm  $\times$  1250 mm were fixed by screws (diameter 3.9 mm, length 45 mm). The space between the two boards was entirely filled with glass wool of  $12.5\text{ kgm}^{-3}$  density.

In this paper two configurations will be discussed. For the first configuration, the gypsum fiber boards were only fixed in each corner by screws at the top and at the bottom of the stud, at a minimum distance of 140 mm off the panels edge. For the other configuration, here called "configuration 4", seven rows of screws were used, with a distance of 307.5 mm between the rows.

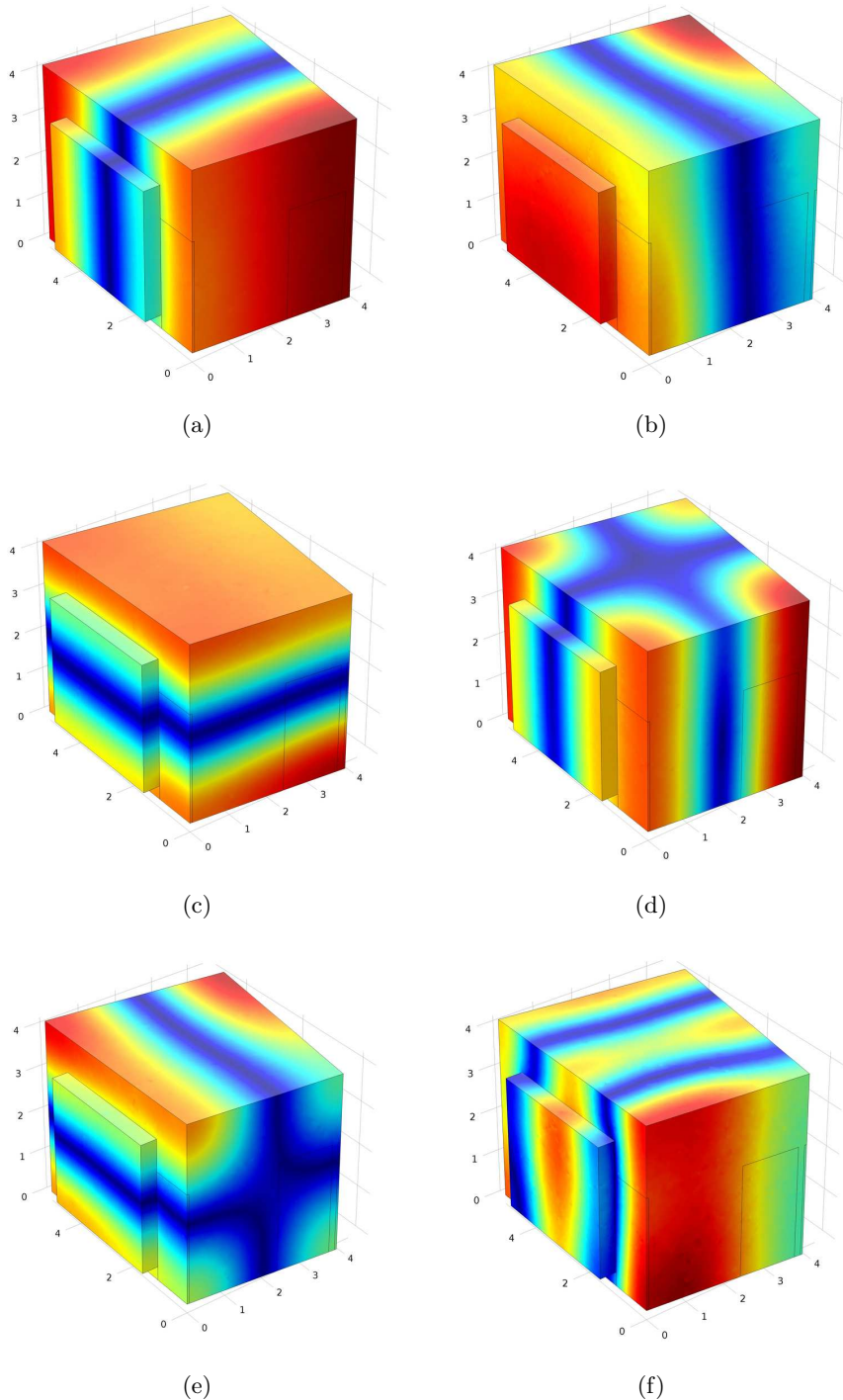


Figure 4: Acoustic eigenmodes of the receiving room, calculated by means of a FEM model. Red and blue colors denote a positive and negative pressure, respectively. The bulge on the front left of each plot corresponds with the location of the test panel. (a) 34.0 Hz; (b) 39.1 Hz; (c) 41.8 Hz; (d) 53.4 Hz; (e) 58.1 Hz; (f) 66.9 Hz.

Note that at the position where the gypsum fiber board butts are joined by means of a dedicated jointing compound, a double column of screws were used for the connection of the boards to the studs, whilst for the stud positions that are not located at such a butt joint only one column of screws was used (c.f. Fig. 5).

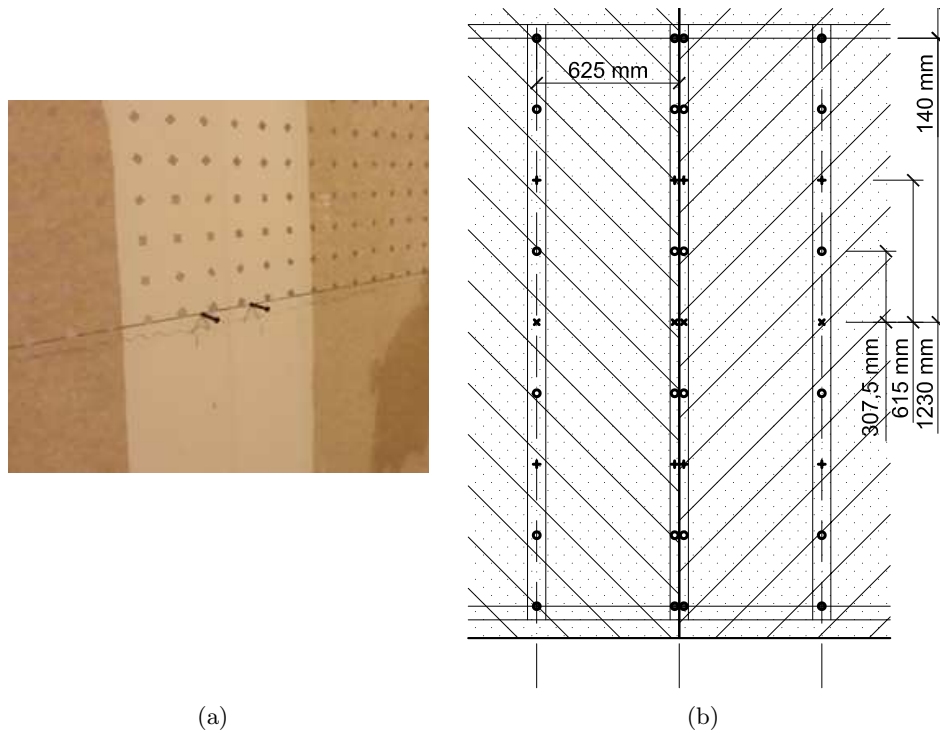


Figure 5: Arrangement of the screws. (a) Photograph of screws to be mounted; (b) mounting details of the gypsum fiber boards.

### 3.2 Measurements of the sound reduction index

The measured sound reduction index  $R$  of the two configurations as a function of frequency, following ISO 10140-2, is shown in Fig. 6.

Figure 6 reveals that the arrangement of the screws (and the tightness with which they are fixed, see [4]) has a considerable influence on the airborne sound insulation properties of the partition.

Configurations differ up to 15 dB, mainly in frequency range from 300 - 4000 Hz.

### 3.3 Laser Doppler vibrometry measurement set-up

A Bruel&Kjaer mini-shaker type 4810 was used to excite the panel mechanically, as shown in Fig. 7(a). The shaker was driven by band limited white noise with a frequency range up to 3000 Hz. It was mounted on the vertical symmetry line of the light-weight structure, between two studs, at the receiving side of the panel using a short stinger. The response of the structure was measured on the same "receive" side of the panel (thus excitation and response measurement is on the same side). The response was measured by means of a scanning laser Doppler vibrometer, as shown in Fig. 7(b). See [4] for further details.

### 3.4 Laser Doppler vibrometry measurement results

In this section the results obtained by data processing of the LDV measurements are presented. Although the laser Doppler vibrometry measurements employed a structure borne excitation at a single point by means of a shaker, it can reveal interesting aspects that also apply to airborne excitation properties of the partition by virtue of the relationship between airborne sound insulation and impact sound pressure level provided by partitions (see [4] for further details).



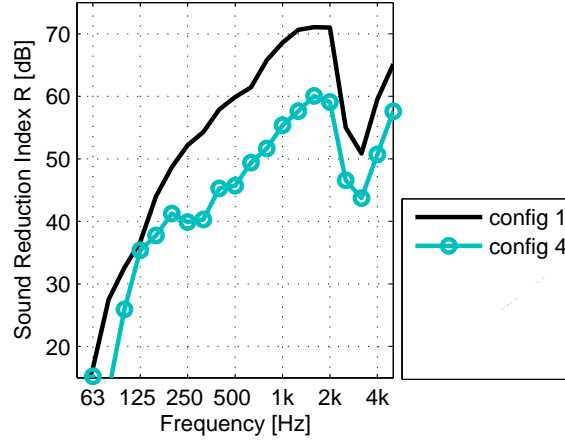


Figure 6: Sound reduction index R of partition with different screw configurations.



(a)



(b)

Figure 7: Measurement equipment. (a) Shaker that was used to excite the wall; (b) scanning laser Doppler vibrometer (developed in-house).

### 3.4.1 Dispersion results

Figure 8 shows a plot of the velocity in the wavenumber domain,  $\hat{v}(\mathbf{k}, \omega)$  for configuration 1 at two frequencies,  $f = \frac{\omega}{2\pi} = 1000$  Hz and 2000 Hz. The wavenumber domain plots for the other configurations and other frequencies are very similar. The plots clearly show circular rings, indicating that the waves propagate at the same velocity in all directions.

Fitting an ellipse through the wavenumber domain results for each measured frequency, using a weighted linear least squares fit, gives an estimate of the wavenumber of the waves propagating in x- and y-direction as a function of frequency, shown in Fig. 9(a) for configuration 1. See [4] for further details. The results are shown in Fig. 9(b) for configuration 1. The propagation velocity turns out to be independent of the propagation direction within experimental uncertainty, inferring perfect elastic isotropy of the gypsum fiber board. Such isotropic behavior was also found for all other configurations. Apparently, the material stress induced by firmly screwing the gypsum fiber board is too weak to induce elastic anisotropy.

The elastic parameters of the gypsum board walls were found by fitting a bending wave model to the measured frequency dependence of the bending wave phase velocity data (Fig. 9(b)) (see [4] for further details).

Fitting the measurement data for configuration 1 on to the bending wave model, optimizing for the Young's modulus  $E$  in a least squares sense, gives the estimates listed in Table 1. Fits of the frequency dependence of the propagation velocities  $c_x$  and  $c_y$  are shown in Fig. 10. The fit on the bending wave model requires knowledge about the density  $\rho$  and the Poisson's ratio  $\nu$ . The weight of the gypsum fibre boards were measured before installation of the boards, from which it followed that the density  $\rho$  was equal to  $1224 \text{ kgm}^{-3}$ . The Poisson's ratio  $\nu$  is assumed

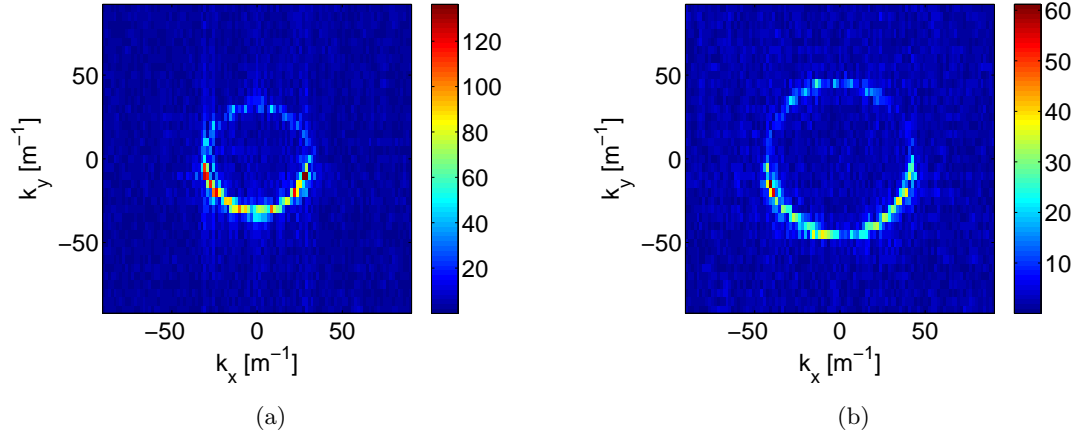


Figure 8: Dispersion plot for configuration 1, showing  $\hat{v}(\mathbf{k}, \omega)$  on a logarithmic scale ( $\log_{10}$  of the absolute value of  $\hat{v}(\mathbf{k}, \omega)$ , arbitrary unit). (a) Frequency = 1000 Hz; (b) frequency = 2000 Hz.

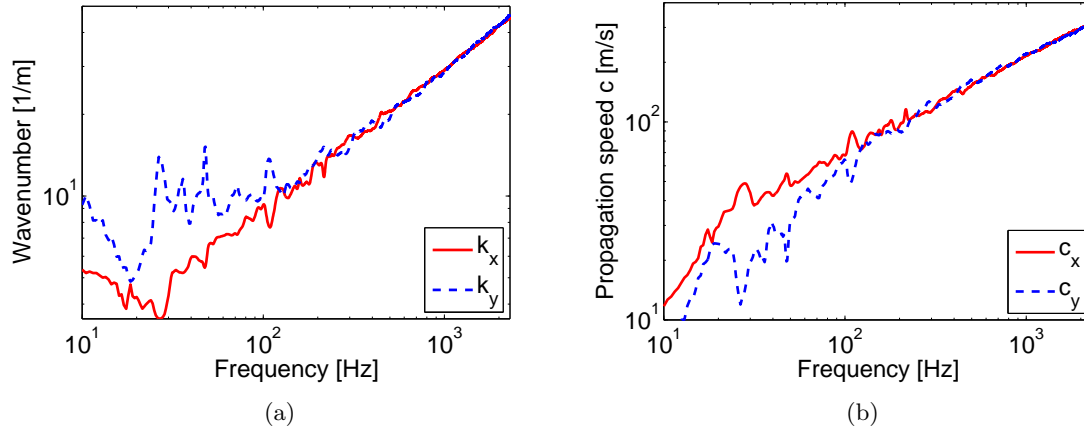


Figure 9: Horizontal and vertical dispersion data obtained by fitting ellipses to the 2D dispersion data of Figure 8. (a) Wavenumbers  $k_x, k_y$ ; (b) propagation velocities  $c_x, c_y$ .

to be equal to 0.3.

The values found for Young's modulus  $E$  are within the range of values (between  $3.5 \cdot 10^9 \text{ Nm}^{-2}$  and  $4.5 \cdot 10^9 \text{ Nm}^{-2}$ ) of the elastic parameters that are stated in the manufacturer's data sheet.

Slightly extrapolating the fit results of the propagation speed  $c_B$  to higher frequencies (Fig. 10), shows that the critical frequency  $f_c$ , for which the bending wave speed equals the speed of sound in air (at  $20^\circ \text{ Celcius}$ :  $343 \text{ ms}^{-1}$ ), is about 2600 Hz in both the  $x$ - and  $y$ -directions. This estimate is confirmed by the measured sound reduction index coincidence dip in the 2500 and 3150 Hz 1/3rd octave bands (Fig. 6).

### 3.4.2 Operational deflection shapes (ODS) analysis

To illustrate the effect of panel fastening, a time domain impulse responses for the two configurations were computed (see [4] for further details). Figure 11 shows an impulse response function due to a 'virtual' impact at the shaker position. The shaker excited a wide range of frequencies, with which the time domain impulse response could be reconstructed with a reasonably good quality. It can be seen that for configuration 1 (screws at bottom and top) the structural waves can freely propagate in the panels. However, for configuration 4 (7 rows of screws firmly fixed)



Physical property		Fit result in x-direction	Fit result in y-direction
$c_L$	$[\text{ms}^{-1}]$	2550	2525
$c_T$	$[\text{ms}^{-1}]$	1170	1160
$E$	$[\text{Nm}^{-2}]$	$4.47 \cdot 10^9 \pm 0.3 \cdot 10^9$	$4.37 \cdot 10^9 \pm 0.5 \cdot 10^9$

Table 1: Fit results using a bending wave model.

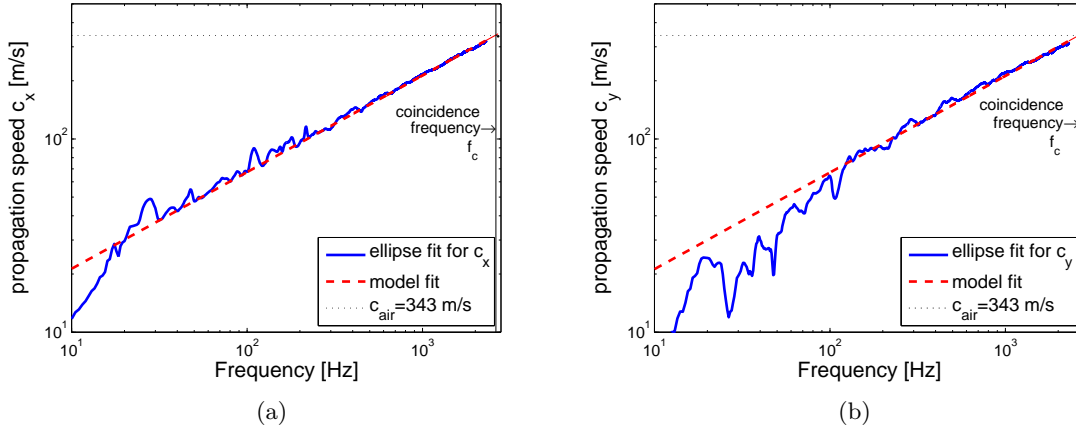


Figure 10: Experimental values (solid line, taken from Figure 9(b)) and fit (dashed curves) for the frequency dependence of the bending wave propagation. The theoretical speed of sound (dotted curve) is indicated, as well as the coincidence frequency  $f_c$ . (a)  $x$ -direction; (b)  $y$ -direction.

the waves are retained in the first two bays which are excited by the shaker directly.

### 3.4.3 Sound power analysis and radiation efficiency analysis

The radiated active sound power was calculated from the LDV measured vibrational panel response by means of a Rayleigh integral, without the influence of the acoustic modes of the receiving room ([3] and Section 2 of this paper). With this model, the radiated sound power and the radiation efficiency of the vibrating building element were determined as a function of frequency. The radiation efficiency for configuration 4 (7 rows of screws firmly fixed) is 2-5 dB higher over a broad frequency range, starting at 500 Hz and upwards up to about 2000 Hz, as compared to configuration 1. The radiation efficiency is presented in 1/24th and 1/3rd octave bands in Fig. 12, showing the same significant differences in radiation efficiency for configuration 4.

The reason of the increased radiation efficiency is because of the increased end-effects due to the fastening of the screws, which causes the acoustic cancellation below the critical frequency to be less effective. Thus it can be concluded that the radiation efficiency is likely to play a comparable role in case of airborne excitation as well, which would partly explain the observed reduction of the sound reduction index  $R$  for some configurations. See [4] for further details.

## 4 CONCLUSIONS

It was shown that the active sound power radiated by a vibrating wall at low frequencies can be determined without the influence of the acoustic modes of the receiving room of a transmission suite, using laser Doppler vibrometry (LDV). The radiated active sound power was calculated from the measurement data by means a Rayleigh integral. The methodology was demonstrated

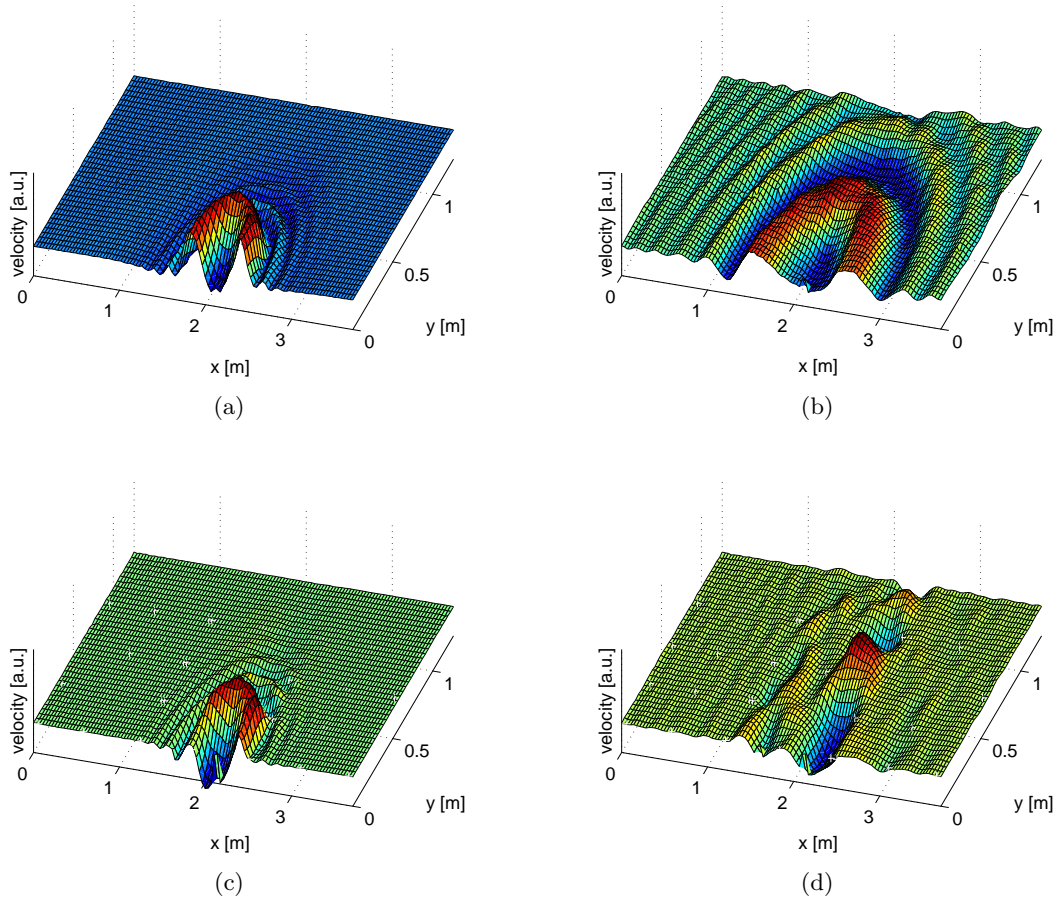


Figure 11: Time domain impulse responses for different configurations. The graphs show the upper half part of the partition only. The + signs denote the position of the screws. (a) Configuration 1, time: 0.0014 s; (b) configuration 1, time: 0.0050 s; (c) Configuration 4, time: 0.0014 s; (d) configuration 4, time: 0.0050 s

for two test walls, a lightweight double wall and a gypsum block wall.

It was also shown that, depending upon the coupling of structural panel modes and acoustic modes of the receiving room, the actual active sound power radiated by the test panel into the receiving room can be significantly influenced. The radiated active sound power of the BEM-based estimate increases at the acoustic resonance frequencies of the receiving room by more than 10 dB, whilst it decreases at non-resonant frequencies, as compared to the free-field radiation (calculated by means of the Rayleigh integral). This is due to the fact that the acoustic impedance that is felt by the vibrating wall is much larger at acoustic resonance frequencies of the receiving room as compared to non-resonant frequencies.

A crucial advantage of the LDV approach is that, by making use of a Rayleigh integral, the intrinsic sound transmission properties of a building element are obtained, independently of the particular properties of the test facility. In addition, uncertainties in the microphone based approaches caused by the spatially varying sound pressure levels at low frequencies as a result of the non-diffuse sound fields in the receiving room, were not encountered when using the LDV approach combined with the Rayleigh integral.

In addition it was shown that the airborne sound insulation of light weight structures are significantly affected by the number of screws used to fasten the panels to the studs. Using the LDV measurement data, the acoustic radiation efficiency and the radiated sound power of the partition were approximated by means of a Rayleigh integral. It was found that rigid fastening of the panels with many screws significant increases the radiation efficiency for structure borne excitation. Using know relations between airborne sound insulation and impact sound pressure

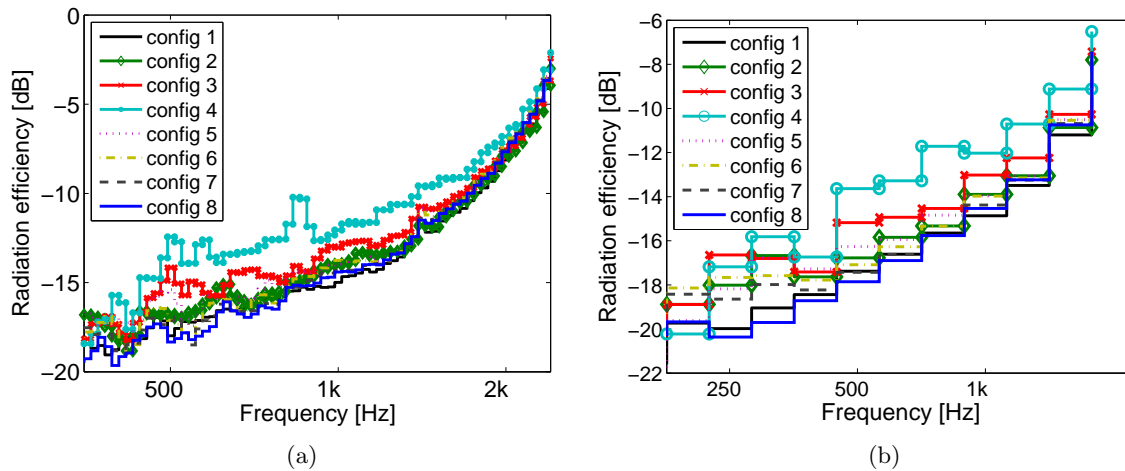


Figure 12: Laser Doppler vibrometry data based calculated radiation efficiency as function of frequency (for a configuration description see Table 1). (a) 1/24th octave band; (b) 1/3rd octave band.

level of a partition, it is argued that this increased radiation efficiency partly explains the reduced sound reduction index for airborne noise as well.

Furthermore, the material properties of the panels were estimated from the dispersion measurements, employing the laser Doppler vibrometry measurement data, resulting in a Young's modulus of approximately  $4.5 \cdot 10^9 \text{ Nm}^{-2}$ , which is very close to the value the manufacturer provided in the data sheet of the panels. From the estimated elastic parameters, the coincidence frequency of the panel was determined as approximately 2600 Hz, which was confirmed by the coincidence dip in the sound reduction index at this frequency.

## Acknowledgements

The Marie Skłodowska-Curie Actions (MSCA) Research and Innovation Staff Exchange (RISE) program (acronym PAPABUILD, proposal number 690970) is acknowledged for its support.

## References

- [1] W. Kropp, A. Pietrzyk, T. Kihlman, On the meaning of the sound reduction index at low frequencies, *Acta Acustica*, Vol. 2, 1994, pp 379-392
- [2] E. Reynders, Parametric uncertainty quantification of sound insulation values, *Journal of the Acoustical Society of America* 135(4)(2014) 1907-1918.
- [3] N.B. Roozen, L. Labelle, M. Rychtáriková, C. Glorieux, Determining radiated sound power of building structures by means of Laser Doppler vibrometry, *Journal of Sound and Vibration*, 2015, DOI: <http://dx.doi.org/10.1016/j.jsv.2015.02.029>, open access: <https://lirias.kuleuven.be/bitstream/123456789/484063/3/Determining+radiated+sound+power+Revision2b.pdf>
- [4] N.B. Roozen, H. Muellner, L. Labelle, M. Rychtáriková, C. Glorieux, Influence of panel fastening on the acoustic performance of light-weight building elements: study by sound transmission and laser scanning vibrometry, *Journal of Sound and Vibration*, 2015, DOI: <http://dx.doi.org/10.1016/j.jsv.2015.02.027>, open access: <https://lirias.kuleuven.be/bitstream/123456789/484064/3/JSVInfluenceofpanelfasteningRev3a.pdf>